Novel cell-free high-throughput screening method for pharmacological tools targeting K^+ channels

Zhenwei Su[a], Emily C. Brown[a], Weiwei Wang[a], and Roderick MacKinnon[a,1]

[a]Laboratory of Molecular Neurobiology and Biophysics, Howard Hughes Medical Institute, The Rockefeller University, New York, NY 10065

Edited by Christopher Miller, Howard Hughes Medical Institute, Brandeis University, Waltham, MA, and approved March 25, 2016 (received for review February 18, 2016)

K^+ channels, a superfamily of ~80 members, control cell excitability, ion homeostasis, and many forms of cell signaling. Their malfunctions cause numerous diseases including neuronal disorders, cardiac arrhythmia, diabetes, and asthma. Here we present a novel liposome flux assay (LFA) that is applicable to most K^+ channels. It is robust, low cost, and high throughput. Using LFA, we performed small molecule screens on three different K^+ channels and identified new activators and inhibitors for biological research on channel function and for medicinal development. We further engineered a hERG (human ether-à-go-go-related gene) channel, which, when used in LFA, provides a highly sensitive (zero false negatives on 50 hERG-sensitive drugs) and highly specific (zero false positives on 50 hERG-insensitive drugs), low-cost hERG safety assay.

liposome flux assay | LFA | K^+ channel screening | hERG safety assay

The K^+ channel superfamily can be divided into five subfamilies, including K_{ir} (inwardly rectifying K^+ channels), K2P (tandem-pore-domain K^+ channels), K_v1–9 (voltage-gated K^+ channels), K_v10–12 [including the hERG (human ether-à-go-go-related gene) channel], and K_{Ca} (Ca^{2+}-activated K^+ channels) (1, 2) (Fig. 1*A*). Their varied structures and gating mechanisms reflect their diverse and important roles in biology. K_{ir} and K2P channels are major regulators of the resting membrane potential. Among K_{ir} channels, K_{ir}3.2 [G protein-activated inwardly-rectifying K^+ channel member 2 (GIRK2)] regulates the electrical excitability of many different neurons in response to inhibitory G protein coupled receptor (GPCR) stimulation (3). K_{ir}6.2 (K-ATP) controls insulin secretion in β cells and is a well-established drug target for diabetes (3). The biological functions of K2P channels remain mostly unknown due to the lack of pharmacological tools. For example, TRAAK (TWIK-related arachidonic acid-stimulated K^+ channel) is biophysically mechanosensitive, but little is known about its biology, especially regarding its mechanosensitivity (4–7). K_v channels repolarize action potentials. Mutations in Kv7.1 (KCNQ1) cause congenital long QT syndrome (2). The hERG channel is the dangerous off-target of many drugs that, by inadvertently inhibiting hERG, cause drug-induced long QT syndrome with the potential of *torsades de pointes* and sudden death (8). High-conductance Ca^{2+}-activated K^+ (Slo1) channel of the K_{Ca} subfamily regulates smooth muscle contraction, and activators of the Slo1 channel are drug candidates for asthma, over-reactive bladder, and hypertension (9–15). These channels are just a small subset of examples illustrating the important roles of K^+ channels to different physiological functions.

Potassium channel pharmacology has contributed greatly to our understanding of K^+ channel mechanisms. In particular, the discovery of naturally occurring peptide toxins isolated from venomous animals, including scorpions, spiders, insects, and snakes, has advanced our understanding of the ion conduction pore and regulatory domains such as voltage sensors (16). Although these toxins have been instrumental to our understanding of certain K^+ channels, there are many K^+ channels—including the entire subfamily of K2P channels—that are insensitive to peptide toxins and for which pharmacological agents are almost nonexistent.

The discovery of small molecule pharmacological agents directed against K^+ channels depends on the availability of a robust, affordable, high-throughput assay. None of the methods currently used—electrophysiology (17, 18), cell-based assays such as Tl^+ flux assays/membrane potential dye assays/yeast growth assays (19–21), and binding/inhibitor competition assays (22, 23)—fulfill all three of the above criteria. We developed and present here an assay that does fulfill these criteria. The assay is based on new methods that allow us to express, purify, and reconstitute virtually any mammalian K^+ channel. Vesicles reconstituted with these channels can be stored frozen for assay at a later date. The assay records K^+ flux across the vesicle membranes, monitored optically with a high signal-to-noise ratio. In this paper, we describe the assay and how it fulfills the criteria of robustness, affordability, and speed. To demonstrate the assay's efficacy we apply it to four K^+ channels, each from a different subfamily. In three channels we identify novel small molecule inhibitors and/or activators. In a fourth channel, hERG, we present a new hERG safety assay and demonstrate its high speed and fidelity.

Results

Assay Description. The principle of the assay is illustrated in Fig. 1*B*. Purified K^+ channels are reconstituted into lipid vesicles in the presence of KCl ranging in concentration from 150 to 300 mM. The channel-containing vesicles are usually frozen for storage at this stage. To assay, thawed vesicles are diluted into a NaCl solution, which creates a strong gradient for the efflux of K^+. Potassium efflux is initiated by the addition of the H^+ ionophore carbonyl cyanide *m*-chlorophenylhydrazone (CCCP), which allows influx of H^+ to counterbalance the efflux of K^+. The H^+ influx is monitored by the H^+-dependent quenching of a fluorescent dye,

Significance

Humans express nearly 80 K^+ channels. This large diversity of K^+ channels (compare 10 Na^+ channels and 10 Ca^{2+} channels) reflects their importance in tying many different biochemical processes to electrical signaling and to shaping and fine-tuning the electrical waveforms produced by excitable cells. We understand the biological roles of only a tiny fraction of the K^+ channels because, for many of them, good pharmacological tools do not exist. To remedy this situation and thus open up a new avenue to study K^+ channels' biological roles, we developed a new cell-free assay that enables the discovery of inhibitors and activators for almost any K^+ channel. It also provides a new high-throughput human ether-à-go-go-related gene safety assay.

Author contributions: Z.S., E.C.B., W.W., and R.M. designed research; Z.S., E.C.B., and W.W. performed research; Z.S., E.C.B., W.W., and R.M. analyzed data; and Z.S., E.C.B., W.W., and R.M. wrote the paper.

The authors declare no conflict of interest.

This article is a PNAS Direct Submission.

See Commentary on page 5472.

[1]To whom correspondence should be addressed. Email: mackinn@rockefeller.edu.

This article contains supporting information online at www.pnas.org/lookup/suppl/doi:10.1073/pnas.1602815113/-/DCSupplemental.

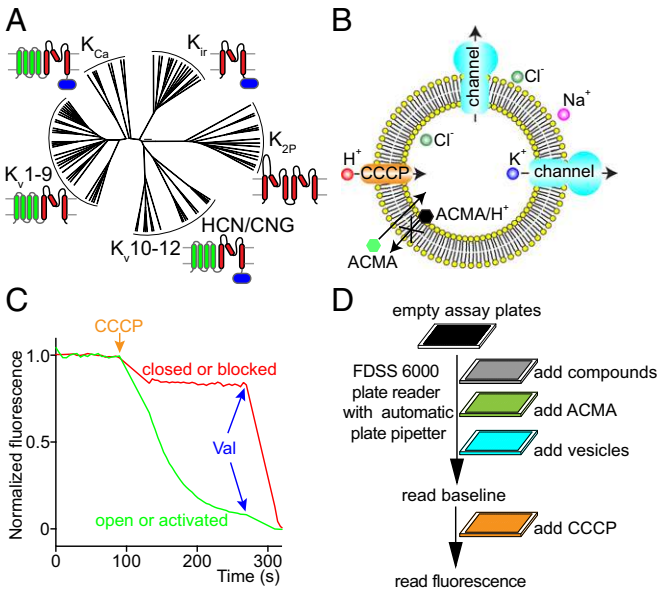

Fig. 1. Introduction to the LFA. (*A*) A phylogenetic tree of human K^+ channels adapted from ref. 4. The K^+ channel superfamily can be divided into five subfamilies, including K_{ir} (inwardly rectifying K^+ channels), K2P (tandem-pore-domain K^+ channels), K_v1–9 (voltage-gated K^+ channels), K_v10–12 (including the hERG channel), and K_{Ca} (Ca^{2+}-activated K^+ channels). K_v10–12 subfamily is related to HCN/CNG channels (hyperpolarization-activated cyclic nucleotide-gated channels/cyclic nucleotide-gated channels). Red highlights the conserved pore domain, green highlights the voltage sensor domain, and blue highlights the intracellular ligand-binding domain. (*B*) A cartoon of the LFA. Purified K^+ channels are reconstituted into lipid vesicles in the presence of high KCl. To assay, thawed vesicles are diluted into a high NaCl solution, which creates a strong gradient for the efflux of K^+. Potassium efflux is initiated by the addition the H^+ ionophore carbonyl cyanide *m*-chlorophenylhydrazone (CCCP), which allows influx of H^+ to counterbalance the efflux of K^+. The H^+ influx is monitored by the H^+-dependent quenching of a fluorescent dye, 9-amino-6-chloro-2-methoxyacridine (ACMA). (*C*) A representative trace of the LFA. K^+ efflux leads to dye quenching when K^+ channels are open (green trace), but not when they are closed or inhibited (red trace). The K^+ ionophore valinomycin (Val) is finally added to allow K^+ channel-independent efflux, to exclude false-positive compounds with strong auto-fluorescence or causing vesicle lysis. (*D*) A cartoon of the cell-free HTS screen procedure. All flux components were added and mixed automatically by FDSS6000 plate reader in sequence as depicted in the figure. Valinomycin, used to induce channel-independent K^+ efflux, was not used in the primary screen on FDSS6000 because it was difficult to wash out and caused contamination among plates.

9-amino-6-chloro-2-methoxyacridine (ACMA). In the example shown in Fig. 1*C*, K^+ efflux leads to dye quenching when K^+ channels are active (green trace), but not when they are inhibited (red trace). The K^+ ionophore valinomycin is finally added to allow K^+ channel-independent efflux. For many K^+ channels, assay conditions under which the channels are inactive can be found to screen for activators that will initiate K^+ efflux. Fig. 1*D* illustrates the sequence of additions used in a multiwell plate format and Fig. 1*C* shows an example of the data readout.

GIRK2. GIRK2 is a K^+ channel that mediates neural inhibition in response to stimulation of $G\alpha_i$-coupled GPCRs. On neurotransmitter stimulation, G protein subunits ($G\beta\gamma$) are released from the receptor, bind to GIRK2, and cause it to open (Fig. 2*A*). The open K^+ channel drives the cell membrane voltage toward the K^+ reversal potential and thus inhibits cellular excitation. In addition to $G\beta\gamma$, GIRK2 activation also requires PIP_2, a signaling lipid, and activation is also modulated by Na^+ (Fig. 2 *A* and *B*). Because GPCR stimulation and multiple intracellular ligands are required to activate GIRK2, cell-based assays will naturally identify many off-target effectors. LFA permits strong biochemical control and is more directed at the channel rather than upstream components of the signaling pathway. Fig. 2 illustrates the biochemical control. When reconstituted in vesicles, GIRK2 channels will incorporate in both directions, inside out and outside out (Fig. 2*B*). By applying $G\beta\gamma$ subunits and a soluble version of PIP_2 outside the vesicles, only inside-out channels become activated. LFA replicates electrophysiological data showing that both $G\beta\gamma$ and PIP_2 are required to robustly activate GIRK2 (Fig. 2*C*). The rate of optical signal response can be controlled to an extent through the GIRK2 protein-to-lipid ratio of vesicles (Fig. S1*A*). This level of fine control enables the use of rate (i.e., slope of the optical signal) as a measure of relative channel activity during inhibitor or activator titrations. Furthermore, titrations of natural ligands such as $G\beta\gamma$ and PIP_2 can be performed with LFA (Fig. S1 *B* and *C*).

To test the ability of LFA to identify small molecules that modify GIRK2 activity, we screened a 100,000 member compound library under two different conditions. First, in the presence of $G\beta\gamma$ and PIP_2 we sought to identify inhibitors. Second, in the absence of $G\beta\gamma$, we sought to identify compounds that could activate GIRK2 by possibly short-circuiting the G protein pathway. Four inhibitors and one activator were identified (Fig. 2*D* and Figs. S2 and S3).

The first inhibitor, RU-GIRK-1, is shown to inhibit GIRK2-mediated flux with an IC50 of about 0.35 μM (Fig. 2*D*). The activity of RU-GIRK-1 was confirmed in an electrophysiological assay in which GIRK2 channels were expressed in cultured cells (Fig. 2*E*). The specificity of this compound for GIRK2 among several K^+ channels, including several other members of the K_{ir} channel subfamily, was also examined (Fig. 2*F*). The compound is also active in a more native context. RU-GIRK-1 inhibits baclofen-stimulated K^+ currents in cultured mouse hippocampal neurons. The compound thus directly confirms the importance of GIRK2 to GPCR-mediated firing of these neurons (Fig. 2*G*).

Three additional inhibitors were identified and characterized (Fig. S2 *A*, *C*, and *E*). Graphs of the slope of the optical signal (relative to the slope in the absence of inhibitor) as a function of compound concentration generated inhibition curves that follow a rectangular hyperbola form. Each of these compounds also inhibited GIRK2 channels in an electrophysiological assay (Fig. S2 *B*, *D*, *F*, and *G*). LFA was also used to assess specificity of these compounds for the GIRK2 channel (Fig. S2*H*).

In the absence of $G\beta\gamma$, LFA identified the antiparasitic agent ivermectin as an apparently G protein-independent activator of GIRK2 (Fig. S3*A*). This activity was confirmed in a whole-cell electrophysiology assay (Fig. S3 *B*–*D*). Although a cell assay alone could not exclude the possibility that ivermectin enhances the action of small quantities of $G\beta\gamma$, LFA was carried out in the complete absence of $G\beta\gamma$. Thus, ivermectin truly appears to short-circuit the G protein signaling pathway.

G protein-independent activation of GIRK2 by ivermectin is interesting because this drug is used in the treatment of parasitic infections, and its major side effect is CNS depression (24, 25). The mechanism of depression is thought to occur through activation of mammalian GABA and glycine receptor Cl^- channels (24, 26–28). However, direct activation of GIRK2 channels in the nervous system could equally contribute to this side effect.

TRAAK. K2P channels are the most extreme structural outliers in the K^+ channel family. Instead of containing four subunits they contain only two, but each has an internal repeat with two K^+ channel signature sequences, providing the required complement of four such sequences to build a K^+ selectivity filter (Figs. 1*A* and 3*A*). K2P channels as a subfamily are the least understood in terms of their biological function. This lack of understanding is due in large part to the paucity of specific K2P channel

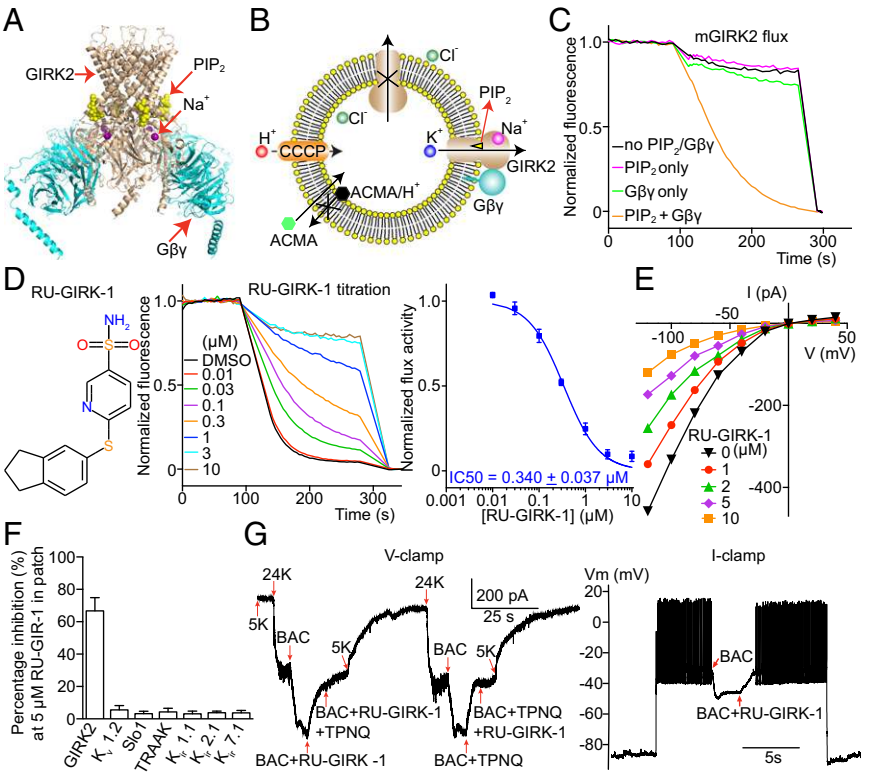

Fig. 2. Mouse GIRK2 screens and characterization of a GIRK2 inhibitor. (*A*) The crystal structure of GIRK2 with PIP_2, Gβγ, and Na^+ bound [Protein Data Bank (PDB) ID code 4KFM]. (*B*) A cartoon showing that GIRK2 ligands applied outside vesicles conveniently activate inside-out facing channels. (*C*) Normalized GIRK2 flux in response to PIP_2 and Gβγ recapitulating electrophysiological recordings. (*D*) (*Left*) RU-GIRK-1 chemical structure. (*Center*) mGIRK2 mediated flux at various concentrations of RU-GIRK-1. (*Right*) Dose–response of RU-GIRK-1 inhibition (n = 9). (*E*) Current-voltage curves from mGIRK2 expressed in HEK293 cells at various RU-GIRK-1 concentrations (n = 3). (*F*) RU-GIRK-1 inhibition of different K^+ channels expressed in cultured cells and recorded using the patch-clamp recording method (n = 3 each). (*G*) (*Left*) A representative voltage-clamp recording of cultured mouse hippocampal neurons with RU-GIRK-1. Extracellular K^+ was increased from 5 to 24 mM to increase K^+ current. GIRK-mediated current was activated by baclofen (BAC), a GABAB receptor agonist; 5 μM RU-GIRK-1 selectively blocked BAC-induced current similar to Tertiapin-Q (TPNQ), a specific peptide toxin for GIRK2. (*Right*) A representative current-clamp recording. Current was injected to depolarize the membrane voltage and induce action potentials. Application of BAC induced hyperpolarization and stopped neuron firing by activating GIRK K^+ current. Subsequent addition of 5 μM RU-GIRK-1 inhibited GIRK current, depolarized the membrane voltage, and restored firing. All data are mean ± SEM.

inhibitors. Our laboratory is working to understand in particular a K2P channel called TRAAK, a mechanosensitive K^+ channel for which no inhibitors have been identified. We identified conditions under which TRAAK yields a robust LFA signal (Fig. S4*A*). We screened 300,000 compounds and identified two inhibitors: RU-TRAAK-1 (Fig. 3*B*) and RU-TRAAK-2 (Fig. S4*B*). These compounds also inhibit TRAAK in electrophysiological assays (Fig. 3 *C*–*E* and Fig. S4 *C* and *D*). RU-TRAAK-1 is poorly reversible, whereas RU-TRAAK-2 is completely reversible. Neither compound inhibits non-K2P channels tested (Kv1.2, Slo1 and GIRK2), but both show some cross-reactivity with certain other members of the K2P subfamily (Fig. 3*E* and Fig. S4*D*). TRAAK's relative resistance to inhibition (only two inhibitors of 300,000 compounds tested) might reflect its unusual structure.

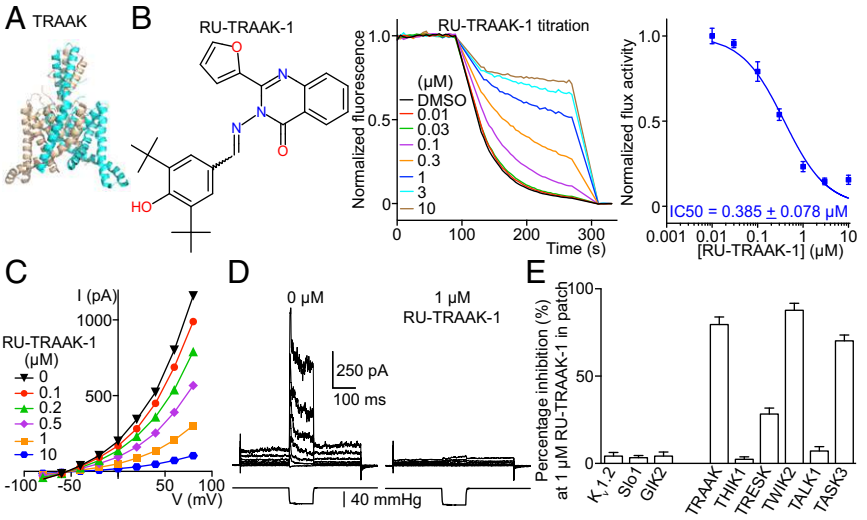

Fig. 3. Characterization of a mouse TRAAK inhibitor. (*A*) A crystal structure of TRAAK (PDB 4I9W). (*B*) (*Left*) RU-TRAAK-1 chemical structure. (*Center*) Normalized LFA efflux curves in the presence of different concentrations of RU-TRAAK-1. (*Right*) Dose–response curve of TRAAK-mediated efflux in the presence of RU-TRAAK-1 (n = 9). (*C*) Whole-cell current-voltage curves from TRAAK expressed in CHO cells in the presence of RU-TRAAK-1 (n = 3). (*D*) One of five recordings of TRAAK in excised patches in the absence and presence of RU-TRAAK-1. Membrane voltage was held at −50 mV, stepped from −80 to +80 mV in 20-mV increments, and returned to −50 mV. In the middle of the voltage protocol, −40 mmHg pressure was applied to the pipette using a pressure clamp to mechanically activate TRAAK; 1 μM RU-TRAAK-1 inhibited both basal current and pressure-stimulated current. (*E*) Channel inhibition by 1 μM RU-TRAAK-1 to test its selectivity in whole-cell recordings (n = 3 each). All data are mean ± SEM.

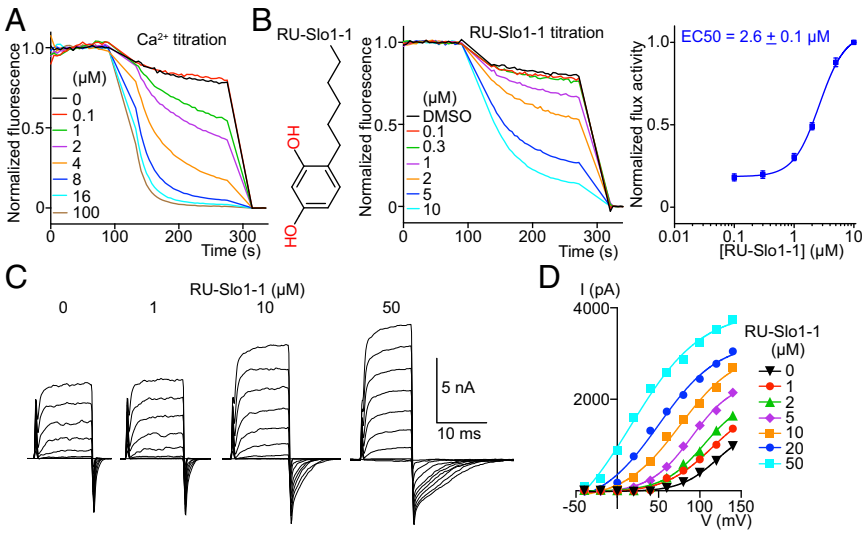

Fig. 4. Characterization of a human Slo1 activator. (*A*) Normalized efflux mediated by Slo1 in response to Ca^{2+}; 1 mM EDTA used for Slo1 small-molecule activator titrations was omitted in the Ca^{2+} titration experiments. (*B*) (*Left*) RU-Slo1-1 chemical structure. (*Center*) Normalized RU-Slo1-1 titration using LFA. (*Right*) Dose–response of RU-Slo1-1 activation (n = 15); 1 mM EDTA was present in RU-Slo1-1 titration. (*C*) A representative inside-out recording of Slo1 expressed in CHO cells at different concentrations of RU-Slo1-1. Channels were held at −40 mV, stepped from −40 to 140 mV in 20-mV increments, and returned to −40 mV. RU-Slo1-1 activated Slo1 by reducing the channel deactivation rate (n = 3). (*D*) A representative current-voltage plot of Slo1 tail current fitted with a Boltzmann equation (n = 3). All data are mean ± SEM.

Compared with most other eukaryotic K^+ channels, TRAAK is relatively small and does not have structured regulatory domains outside the membrane that would create opportunity for binding small inhibitory molecules. We anticipate that these inhibitors, applied in well-controlled experiments, will offer new information on the biological roles of TRAAK channels.

High Conductance Ca^{2+}-Activated K^+ Channel. High conductance Ca^{2+}-activated K^+ channel, here referred to as Slo1, regulates smooth muscle tone and several other cellular processes related to feedback inhibition by intracellular Ca^{2+}. Human mutations that cause asthma and mouse genetic and pharmacological studies suggest that Slo1 activators might provide benefit in the treatment of asthma, hypertension and over-reactive bladder (9–15). We thus applied LFA to the Slo1 channel to identify molecules that would open the channel. A control experiment shows that the natural intracellular ligand, Ca^{2+}, opens the channel and induces K^+ flux in LFA (Fig. 4*A*). A channel opener (i.e., activator) screen was run at subthreshold Ca^{2+} concentrations (1.0 mM EDTA); 300,000 compounds were assayed and seven activators belonging to five distinct chemical categories were identified (Fig. 4*B* and Fig. S5 *A*, *C*, *E*, *G*, *I*, and *K*). One of these—RU-Slo1-2—was previously identified as a Slo1 activator (29). Each of these compounds were further examined in an electrophysiology assay for their ability to activate Slo1 at very low Ca^{2+} concentrations (Fig. 4 *C* and *D* and Fig. S5 *B*, *D*, *F*, *H*, *J*, and *L*). Because Slo1 is also a voltage-dependent K^+ channel, it can open at low Ca^{2+} concentrations as long as that the membrane is sufficiently depolarized (i.e., voltage on the inside is made very positive relative to outside; Fig. 4*C*). We found that all activators promote channel opening at less depolarizing voltages (Fig. 4 *C* and *D* and Fig. S5 *B*, *D*, *F*, *H*, *J*, and *L*). Ca^{2+} is known to have precisely this effect (30). Therefore, the activators appear to mimic the effect of Ca^{2+} on the Slo1 channel. Such compounds have the potential to induce smooth muscle relaxation by opening Slo1 channels and hyperpolarizing the membrane.

hERG. The hERG channel is present in cardiac cells where it participates in repolarization of the action potential. When hERG function is impeded, a characteristic lengthening of the Q-T interval is detectable on the electrocardiogram of mammals. This phenomenon is associated in humans with a lethal arrhythmia called *torsade de pointes*. For a reason that is not well understood, the hERG channel is highly susceptible to block by many structurally diverse small molecules. Our ability to predict which small molecules will block hERG is poor and therefore all compounds under consideration for drug development are tested in a hERG activity assay. Several assays exist: cell-based functional assays, such as thallium and/or rubidium flux, nonfunctional assays, such as ligand binding and/or fluorescence polarization, and electrophysiology (22, 23, 31, 32). The gold standard is electrophysiology, but it can be slow and expensive when the need exists for evaluating many compounds.

We applied LFA to the hERG channel. We first had to solve how to produce sufficient quantities of a stable version of this human K^+ channel because the native, full-length channel aggregates when purified. Through trial and error we discovered that if we modified the amino acid sequence by deleting two different intracellular loops we could purify a biochemically well-behaved hERG channel with good function and correct pharmacology (Fig. 5). The behavior in LFA of two well-known hERG channel blockers, dofetilide and astemizole, is shown (Fig. 5 *C*–*E*). These drugs inhibit flux as predicted on the basis of electrophysiology assays (31, 33).

To test the sensitivity of an LFA-based hERG safety assay, we examined 50 known inhibitors at a concentration of 10^{-5} M and obtained zero false negatives (Fig. S6 and Table S1). A complete dose–response relation was determined for all 50 hERG channel blockers (Fig. S6 and Table S1). A plot showing IC50 values determined using LFA against IC50 values using electrophysiology reported in the literature shows that LFA correlates well with electrophysiology-determined values (Fig. 5*F*). We note that the IC50 determined by LFA for hERG blockers is, on average, approximately 10 times higher (i.e., lower affinity) than the IC50 determined by electrophysiology. The origin of this offset is due mainly to the following property of the LFA assay: K^+ efflux is coupled to H^+ influx and for some channels such as hERG the latter is rate limiting until K^+ channels are mostly inhibited. Therefore, IC50 in LFA corresponds to a percentage of channel inhibition much higher than 50%, which leads to the IC50 offset observed (Fig. 5 *F* and *G*. Also see Methods for a detailed explanation). Thus, we consider

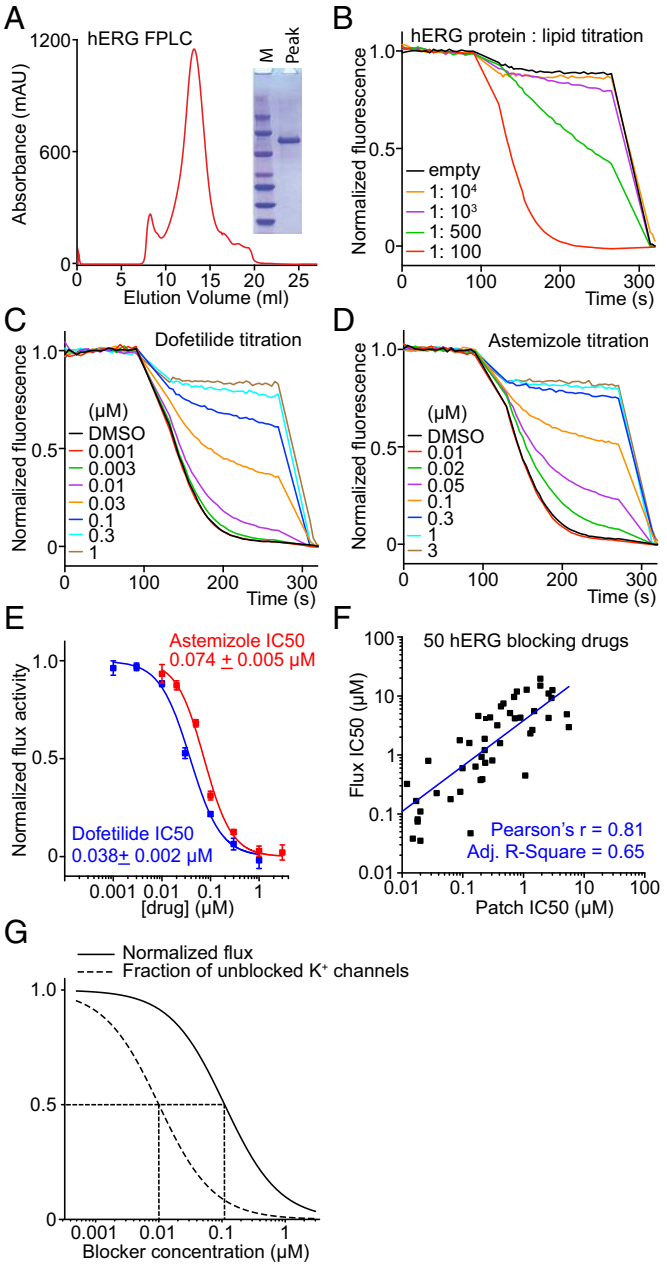

Fig. 5. Development and validation of a new hERG assay. (*A*) A hERG mutant channel with internal deletions of unstructured cytoplasmic loops (residues 141–380 and 871–1005) was engineered. This mutant channel protein ran as a monodisperse FPLC peak on gel filtration and as a single band on SDS/PAGE. (*B*) Protein-to-lipid ratio titration of hERG in LFA showing that 1:100 provided a good signal for drug safety testing. (*C* and *D*) Normalized titration of dofetilide and astemizole, two well-characterized hERG blockers. The LFA IC50 values correlate well with electrophysiological recordings, although are around 10-fold higher (*Methods*). (*E*) Dose–response curves derived from LFA (n = 3 each). (*F*) LFA IC50 values were plotted against patch recording IC50 values reported in the literature (the lowest affinity IC50 values were used if a range of IC50 values were reported by patch clamp). No false negatives were found. The plot was fitted with linear regression in OriginPro. All data are mean ± SEM. (*G*) Simulation of LFA recorded normalized flux (solid curve) and fraction of unblocked K^+ channels (dashed curve) as a function of blocker concentration (*Methods*).

LFA a semiquantitative high throughput assay for rapid identification of hERG blockers. Once an inhibitor is identified, the IC50 can then be confirmed using an electrophysiology assay.

To test the assay's specificity we examined 50 known non-inhibitors (34) at the same concentration and obtained a zero false-positive rate (Fig. S7 and Table S2). On repeat at 10 times higher concentration (approaching the solubility of many drugs), less than 25% inhibition was observed compared with a DMSO control (Table S2).

The data shown in this study were carried out using 384-well plates; however, an example using a 1,536-well plate with a similarly high signal demonstrates the ease with which the assay can be scaled (Fig. S8).

Discussion

The K^+ channel family comprises a structurally and functionally diverse class of ion channels. All members share a similar pore but their gating mechanisms vary enormously. That is presumably why we observe close to 80 K^+ channels encoded in the human genome, to allow regulation of K^+ permeability by a myriad of intracellular ligands, lipids, membrane voltage, and membrane stretch. We still do not understand the biological roles played by many of these channels, mainly because we have not yet developed a sufficient set of pharmacological tools. Gene knockout technology has advanced our understanding to some degree, but such approaches are not good surrogates for acute pharmacology experiments because compensatory expression of a second channel that can fulfill the role of the missing first is all too common, especially given the large number and redundancy of K^+ channels (35, 36).

This paper presents an assay called LFA, to identify inhibitors and activators of K^+ channels. LFA is made possible by methods that now permit the expression and purification of almost any mammalian K^+ channel. We developed this assay to identify pharmacological agents to study the biological roles of many still poorly understood K^+ channels. To our knowledge, we identified the first inhibitors of TRAAK and new activators of Slo1. We also discovered that the antiparasitic agent ivermectin activates GIRK2 in an apparently G protein-independent manner. This action could potentially underlie a major side effect of this drug, to induce CNS depression.

These data also suggest that LFA may also be useful for drug development purposes. Fluorescence baseline and initial slope measurements, which are used to quantify flux activity, can be made in parallel on a plate reader in a 2-min interval. Therefore, a 1,536-well plate reader can potentially record about one million measurements per day. Although our laboratory typically runs the assay in a 384-well format, we demonstrated the strong signal measured using 1,536-well plates (Fig. S8) and therefore the assay is easily scalable. Human genetic data point to K^+ channels as being likely targets for new therapies for asthma (9, 11, 13), hypertension (15, 37), and perhaps even anticancer therapy (38). LFA can allow rapid screening for identifying new compounds that target K^+ channels.

A hERG safety assay based on LFA seems to provide data similar in quality to an electrophysiology assay but at an incomparably higher rate and a tiny fraction of the cost. LFA could easily quantify hERG activity in the vast number of derivative compounds that can be generated through combinatorial synthesis. Such capability would help in efforts to chemically remove hERG activity and realize the potential benefit of a drug.

Methods

Detailed materials and methods are presented in *SI Methods*.

Protein Purifications. Mouse GIRK2 was expressed and purified from *Pichia pastori* yeast cells. Human Gβγ complex was expressed and purified from High Five insect cells. Mouse TRAAK was expressed and purified from *P. pastori* yeast cells. Human Slo1 was expressed and purified from Sf9 (*Spodoptera frugiperda*) insect cells. hERG was expressed and purified from HEK293S GnTI$^-$ mammalian cells.

Proteoliposome Reconstitution. Purified proteins were reconstituted into POPE (1-palmitoyl-2-oleoyl-sn-glycero-3-phosphoethanolamine) and POPG [1-palmitoyl-2-oleoyl-sn-glycero-3-phospho-(1'-rac-glycerol)] vesicles [with a ratio of 3:1 (wt:wt)] by a dialysis method.

High-Throughput LFA Screens. A 300,000 compound library was constructed from Enamine, Chembridge, and Rockefeller chemical library sources. The primary screen was carried out with a FDSS6000 (Hamamatsu) plate reader with automatic pipetting in 384-well format. The FDSS6000 pipetted and mixed 12 μL compound solution, 6 μL ACMA solution, and 6 μL vesicle solution into an assay plate, and the baseline fluorescence was recorded. Then, 6 μL CCCP was added and mixed to initiate the K^+ flux, and the fluorescent signal was monitored every 5 s for 55 cycles. The final concentrations for the components in the LFA reaction were 1 μM compound, 1.3 μM ACMA, and 3.2 μM CCCP.

Hit Confirmation Using LFA. Once the primary screens were finished and primary hits were selected using offline data analysis, the hits were confirmed using a fluorescent plate reader (Tecan, Infinite M1000 with excitation wavelength 410 nm and emission wavelength 490 nm) with manual pipetting following the same protocol as the primary screen in 384-well plates. Confirmed hits were purchased freshly from the same vendors that had supplied the primary screening compounds and drug titrations were conducted. The flux data were normalized, plotted, and fitted as detailed in *SI Methods*.

Animals. All animal protocols were approved by the IACUC (Institutional Animal Care and Use Committee) of The Rockefeller University. Newborn C57BL/6J mice (The Jackson Laboratory) were killed for the dissection of hippocampal neurons.

Hippocampal Neuron Cultures. Hippocampus tissues were dissected from P0 neonatal mice in cold Hank's balanced salt solution without Ca^{2+} and Mg^{2+}. Dissected tissues were digested by trypsin, gently triturated, and plated on poly-D-lysine– and laminin-coated coverslips. Neurons matured after 1 wk after plating and were patched between 1 and 2 wk.

Plasmid Transfection. HEK293 or CHO cells were cultured to 80% confluency and transfected with Lipofectamine 2000. Cells were treated with trypsin and plated out on coverslips 12–24 h after transfection and patched 6–48 h after plating.

Electrophysiology. Different channel constructs were expressed in HEK293 or CHO cells and patched using standard whole-cell or excised configuration.

Data Analysis. All data are presented as mean ± SEM.

ACKNOWLEDGMENTS. We thank J. Fraser Glickman, Antonio Luz, and Jeanne Chiaravalli-Giganti at the High-Throughput and Spectroscopy Resource Center of The Rockefeller University for assistance with the screens; Maria L. Garcia and Gregory J. Kaczorowski for advice with data analyses; Stephen G. Brohawn for assistance with K2P constructs and TRAAK purification; Yi Chun Hsiung for assistance with insect and mammalian cell cultures; and members of the R.M. laboratory for helpful discussions. R.M. is an investigator in the Howard Hughes Medical Institute. Other funding support includes National Institutes of Health Grant GM43949, American Asthma Foundation extension award, The Robertson Therapeutic Development Fund, and The Bridge Fund (to R.M.).

1. Yu FH, Yarov-Yarovoy V, Gutman GA, Catterall WA (2005) Overview of molecular relationships in the voltage-gated ion channel superfamily. *Pharmacol Rev* 57(4):387–395.
2. Shieh C-C, Coghlan M, Sullivan JP, Gopalakrishnan M (2000) Potassium channels: Molecular defects, diseases, and therapeutic opportunities. *Pharmacol Rev* 52(4):557–594.
3. Hibino H, et al. (2010) Inwardly rectifying potassium channels: Their structure, function, and physiological roles. *Physiol Rev* 90(1):291–366.
4. Brohawn SG, del Mármol J, MacKinnon R (2012) Crystal structure of the human K2P TRAAK, a lipid- and mechano-sensitive K^+ ion channel. *Science* 335(6067):436–441.
5. Brohawn SG, Su Z, MacKinnon R (2014) Mechanosensitivity is mediated directly by the lipid membrane in TRAAK and TREK1 K^+ channels. *Proc Natl Acad Sci USA* 111(9):3614–3619.
6. Brohawn SG, Campbell EB, MacKinnon R (2014) Physical mechanism for gating and mechanosensitivity of the human TRAAK K^+ channel. *Nature* 516(7529):126–130.
7. Honoré E (2007) The neuronal background K2P channels: Focus on TREK1. *Nat Rev Neurosci* 8(4):251–261.
8. Vandenberg JI, et al. (2012) hERG K^+ channels: Structure, function, and clinical significance. *Physiol Rev* 92(3):1393–1478.
9. Nardi A, Olesen S-P (2008) BK channel modulators: A comprehensive overview. *Curr Med Chem* 15(11):1126–1146.
10. Ponte CG, et al. (2012) Selective, direct activation of high-conductance, calcium-activated potassium channels causes smooth muscle relaxation. *Mol Pharmacol* 81(4):567–577.
11. Semenov I, Wang B, Herlihy JT, Brenner R (2006) BK channel beta1-subunit regulation of calcium handling and constriction in tracheal smooth muscle. *Am J Physiol Lung Cell Mol Physiol* 291(4):L802–L810.
12. Bentzen BH, Olesen S-P, Rønn LCB, Grunnet M (2014) BK channel activators and their therapeutic perspectives. *Front Physiol* 5:389.
13. Seibold MA, et al. (2008) An african-specific functional polymorphism in KCNMB1 shows sex-specific association with asthma severity. *Hum Mol Genet* 17(17):2681–2690.
14. Petkov GV, et al. (2001) β1-subunit of the Ca^{2+}-activated K^+ channel regulates contractile activity of mouse urinary bladder smooth muscle. *J Physiol* 537(Pt 2):443–452.
15. Eichhorn B, Dobrev D (2007) Vascular large conductance calcium-activated potassium channels: Functional role and therapeutic potential. *Naunyn Schmiedebergs Arch Pharmacol* 376(3):145–155.
16. Mouhat S, Andreotti N, Jouirou B, Sabatier J-M (2008) Animal toxins acting on voltage-gated potassium channels. *Curr Pharm Des* 14(24):2503–2518.
17. Schroeder K, Neagle B, Trezise DJ, Worley J (2003) Ionworks HT: A new high-throughput electrophysiology measurement platform. *J Biomol Screen* 8(1):50–64.
18. Dunlop J, Bowlby M, Peri R, Vasilyev D, Arias R (2008) High-throughput electrophysiology: An emerging paradigm for ion-channel screening and physiology. *Nat Rev Drug Discov* 7(4):358–368.
19. Beacham DW, Blackmer T, O' Grady M, Hanson GT (2010) Cell-based potassium ion channel screening using the FluxOR assay. *J Biomol Screen* 15(4):441–446.
20. Whiteaker KL, et al. (2001) Validation of FLIPR membrane potential dye for high throughput screening of potassium channel modulators. *J Biomol Screen* 6(5):305–312.
21. Bagriantsev SN, et al. (2013) A high-throughput functional screen identifies small molecule regulators of temperature- and mechano-sensitive K2P channels. *ACS Chem Biol* 8(8):1841–1851.
22. Priest B, Bell IM, Garcia M (2008) Role of hERG potassium channel assays in drug development. *Channels* 2(2):87–93.
23. Huang X-P, Mangano T, Hufeisen S, Setola V, Roth BL (2010) Identification of human Ether-à-go-go related gene modulators by three screening platforms in an academic drug-discovery setting. *Assay Drug Dev Technol* 8(6):727–742.
24. Trailovic SM, Nedeljkovic JT (2011) Central and peripheral neurotoxic effects of ivermectin in rats. *J Vet Med Sci* 73(5):591–599.
25. Geyer J, Janko C (2012) Treatment of MDR1 mutant dogs with macrocyclic lactones. *Curr Pharm Biotechnol* 13(6):969–986.
26. Adelsberger H, Lepier A, Dudel J (2000) Activation of rat recombinant $\alpha_1\beta_2\gamma_{2S}$ $GABA_A$ receptor by the insecticide ivermectin. *Eur J Pharmacol* 394(2-3):163–170.
27. Shan Q, Haddrill JL, Lynch JW (2001) Ivermectin, an unconventional agonist of the glycine receptor chloride channel. *J Biol Chem* 276(16):12556–12564.
28. Lynagh T, Lynch JW (2012) Molecular mechanisms of Cys-loop ion channel receptor modulation by ivermectin. *Front Mol Neurosci* 5:60.
29. Nausch B, et al. (2014) NS19504: A novel BK channel activator with relaxing effect on bladder smooth muscle spontaneous phasic contractions. *J Pharmacol Exp Ther* 350(3):520–530.
30. Cox DH, Cui J, Aldrich RW (1997) Allosteric gating of a large conductance Ca-activated K^+ channel. *J Gen Physiol* 110(3):257–281.
31. Guo L, Guthrie H (2005) Automated electrophysiology in the preclinical evaluation of drugs for potential QT prolongation. *J Pharmacol Toxicol Methods* 52(1):123–135.
32. Piper DR, et al. (2008) Development of the predictor HERG fluorescence polarization assay using a membrane protein enrichment approach. *Assay Drug Dev Technol* 6(2):213–223.
33. Rampe D, Roy ML, Dennis A, Brown AM (1997) A mechanism for the proarrhythmic effects of cisapride (Propulsid): High affinity blockade of the human cardiac potassium channel HERG. *FEBS Lett* 417(1):28–32.
34. Wible BA, et al. (2005) HERG-Lite: A novel comprehensive high-throughput screen for drug-induced hERG risk. *J Pharmacol Toxicol Methods* 52(1):136–145.
35. Parrish JZ, et al. (2014) Krüppel mediates the selective rebalancing of ion channel expression. *Neuron* 82(3):537–544.
36. Hao J, et al. (2013) Kv1.1 channels act as mechanical brake in the senses of touch and pain. *Neuron* 77(5):899–914.
37. Ji W, et al. (2008) Rare independent mutations in renal salt handling genes contribute to blood pressure variation. *Nat Genet* 40(5):592–599.
38. Huang X, Jan LY (2014) Targeting potassium channels in cancer. *J Cell Biol* 206(2):151–162.
39. Goehring A, et al. (2014) Screening and large-scale expression of membrane proteins in mammalian cells for structural studies. *Nat Protoc* 9(11):2574–2585.
40. Kawate T, Gouaux E (2006) Fluorescence-detection size-exclusion chromatography for precrystallization screening of integral membrane proteins. *Structure* 14(4):673–681.
41. Rothbauer U, et al. (2008) A versatile nanotrap for biochemical and functional studies with fluorescent fusion proteins. *Mol Cell Proteomics* 7(2):282–289.
42. Fridy PC, et al. (2014) A robust pipeline for rapid production of versatile nanobody repertoires. *Nat Methods* 11(12):1253–1260.